Stable microwave oscillations due to external-cavity-mode beating in laser diodes subject to optical feedback

T. Erneux,[1] A. Gavrielides,[2] and M. Sciamanna[3,*]
[1]*Optique Nonlinéaire Théorique, Université Libre de Bruxelles, Campus Plaine C.P. 231, 1050 Bruxelles, Belgium*
[2]*Nonlinear Optics Center, Air Force Research Laboratory, 3550 Aberdeen Avenue S.E., Kirtland AFB, New Mexico 87117-5776*
[3]*Service d'Electromagnétisme et de Télécommunications, Faculté Polytechnique de Mons, Boulevard Dolez 31, 7000 Mons, Belgium*
(Received 17 May 2002; published 17 September 2002)

Laser diodes subject to a delayed optical feedback may exhibit high-frequency oscillating intensities as a result of a beating between two external-cavity-modes (ECMs). We analyze the conditions for the stability of these microwave oscillations in the framework of the Lang-Kobayashi equations for a single-mode edge-emitting semiconductor laser [R. Lang and K. Kobayashi, IEEE J. Quantum Electron. **QE-16**, 347 (1980)]. We show that two different scenarios are possible. If the linewidth enhancement factor is relatively large ($\alpha=2-5$), the beating occurs between a stable ECM (mode) and an unstable ECM (antimode). The stability of the time-periodic solution is then limited in parameter space. But if the linewidth enhancement factor is sufficiently low ($\alpha\leqslant\alpha_c\simeq 1$), a beating between two stable modes is possible allowing stable high-frequency oscillating outputs.

DOI: 10.1103/PhysRevA.66.033809 PACS number(s): 42.65.Sf, 05.45.−a

I. INTRODUCTION

Semiconductor lasers subject to optical feedback from an external cavity (EC) exhibit a variety of instabilities depending on the values of the laser parameters such as the EC length, the feedback strength, or the pump parameter. The coherence collapse regime [1] typically occurs in systems with sufficiently long (1 cm and more) ECs. Beyond a critical feedback rate, we note a sudden increase in linewidth as well as a drastic increase in the relative intensity noise. Coherence collapse results from the interaction between the laser relaxation oscillation frequency and the EC mode (ECM) frequencies. Its chaotic dynamics has been widely studied [2–5]. It disappears for short ECs (typically less than 5 mm) as the ECM spacing becomes much larger than the laser relaxation oscillation frequency.

However, Tager and Elenkrig (1993) [6] and Tager and Petermann (1994) [7] found that another instability is possible for short ECs that results from a beating between two ECMs. They studied the Lang-Kobayashi (LK) equations [8] that describe the dynamics of a single-mode edge-emitting laser subject to a weak to moderate optical feedback. By numerical simulations and linear stability arguments, they showed that an oscillatory instability resulting from the beating of two ECMs could lead to an efficient source in the microwave (>20 GHz) region. The work by Tager and Petermann [7] on short ECs was motivated by the effects of optical feedback due to reflection at fiber pigtails, in optical fiber connectors. It led to interesting guidelines for the design of high-speed laser diodes with an integrated passive cavity where the EC is typically short [9].

Analytical studies of the LK equations [10] have yielded insight into this beating regime between ECMs. In addition to the single-ECM solutions, two-ECM solutions of the LK equations are possible. Of particular engineering interest is the fact that these two-ECM solutions exhibit a rapidly oscillating intensity. The oscillations clearly result from a beating between two single-ECMs and the frequency is proportional to the inverse of the external-cavity round-trip time. The two-ECM solutions appear through a Hopf bifurcation bridge connecting a stable ECM (mode) and an unstable saddle-type ECM (antimode). This means that the high-frequency outputs for the parameters considered in Refs. [6,7] are only partially stable.

This raises the important question of the stability of a two-ECM solution. Is a stable beating between two ECMs possible in a semiconductor laser subject to optical feedback? In this paper, we show that this is indeed the case for particular values of the laser parameters. Using the LK equations, we determine analytical conditions for a stable beating and we test our results by using a numerical continuation method for delay differential equations [11].

The existence of high-frequency two-ECM regimes has motivated a series of recent experimental and theoretical studies. First, the beating between a mode and an antimode found for short ECs also appear for long ECs [12]. Second, experimental observations of two-ECM regimes were possible for an edge-emitting laser subject to two optical feedbacks [13–15]. The mixed mode regime was shown to be partially stable and quasiperiodic outputs leading to low-frequency fluctuations (LFF) were observed after its destabilization [15], in good agreement with the theory [10,12]. LFF consists of irregular fluctuations of the laser intensity on microsecond to nanosecond time scales. These time scales are long compared to the laser relaxation oscillation period and the external-cavity round-trip time. Third, high-frequency oscillations have been experimentally observed in vertical-cavity surface-emitting lasers (VCSELs) subject to a polarization rotating optical feedback [16]. Systematic numerical

*Corresponding author;
Electronic address: Sciamanna@ telecom.fpms.ac.be

bifurcation studies of the rate equations [17,18] have revealed that these oscillations result from the interaction between two stable ECMs (modes). In all these experimental and theoretical studies, only partially stable microwave oscillations were reported. In this paper, we examine the bifurcation diagram of the LK equations and determine the conditions for stable microwave oscillations. Our analysis is based on the stability properties of a particular point (called a two-ECM point) at which two single-ECM solutions exhibit identical intensities. Delayed laser systems admitting a large number of ECMs, such as the double cavity or the VCSEL system, exhibit many of these two-ECM points and are good candidates for efficient sources of stable microwave oscillations.

The plan of the paper is as follows. In Sec. II, we introduce the dimensionless LK equations [8] describing a semiconductor laser exposed to optical feedback from a flat external mirror. The typical values of the photon and carrier density decay rates then motivate an asymptotic analysis of these equations. We omit all mathematical details for clarity. In Sec. III, we discuss the leading order conditions for a two-ECM beating in terms of the linewidth enhancement factor. We find that a stable beating is always possible if the linewidth enhancement factor is sufficiently low. Our conclusions are tested numerically in Sec. IV by determining the bifurcation diagram of the steady and time-periodic intensity solutions.

II. FORMULATION, EXTERNAL CAVITY MODES, AND BEATING BETWEEN MODES

The LK equations [8] describe a single longitudinal mode edge-emitting laser subject to a weak to moderate external optical feedback. Previous theoretical and numerical studies of these equations (see Ref. [19] and references therein) have shown that we may benefit from the relative order of magnitudes of the laser parameters. They motivate asymptotic theories of the LK equations leading to simplified problems. The solutions of these problems highlight specific bifurcation scenarios responsible for the laser rich dynamics. The starting point of any asymptotic analysis is to write dimensionless equations. The LK dimensionless rate equations are two equations for the electrical field Y and the excess carrier number Z given by [20]

$$\frac{dY}{ds}=(1+i\alpha)ZY+\eta\exp(-i\omega\theta)Y(s-\theta), \tag{1}$$

$$T\frac{dZ}{ds}=P-Z-(1+2Z)|Y|^2. \tag{2}$$

In these equations, time s is measured in units of the photon lifetime τ_p ($s\equiv t/\tau_p$). The parameters T and θ are defined as $T\equiv\tau_n/\tau_p$ and $\theta\equiv\tau/\tau_p$ where τ_n and τ are the carrier lifetime and the external round-trip time, respectively, $\omega\equiv\omega_0\tau_p$ is the angular frequency of the solitary laser ω_0 normalized by τ_p^{-1}, $\eta\equiv\gamma\,\tau_p$ is the feedback rate γ normalized by τ_p^{-1}, P represents the excess pump current and α is the linewidth enhancement factor, and T is typically an $O(10^3)$ large parameter for semiconductor lasers. Equation (2) then suggests that Z is a function of the slow time variable $T^{-1}s$. We shall take advantage of this observation in our analysis.

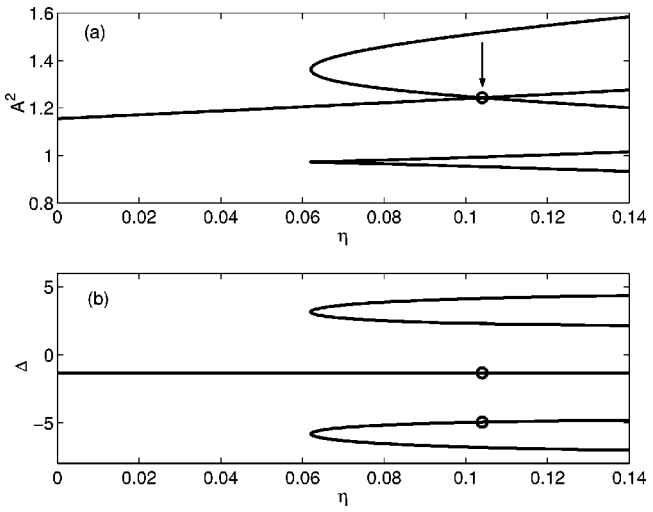

FIG. 1. Bifurcation diagram of the first two single-ECM solutions. Figures (a) and (b) show the intensity $|Y|^2=A^2$ and the frequency $\Delta=\sigma\theta$ of each ECM. They are obtained by changing Δ and computing $\eta\theta$ and A from Eqs. (4) and (5), respectively. The arrow in Fig. 1(a) indicates the point where the two single ECMs admit the same intensity and is called a two-ECM point. The values of the parameters are $P=1.155$, $\theta=18$, $\alpha=4$, and $\omega\theta=-\arctan(\alpha)$. The first ECM frequency is constant ($\Delta_1=\omega\theta$) while the second ECM frequency emerges from a limit point. At the two-ECM point $\Delta_2=-\Delta_1-2\pi$.

A basic solution of the LK equations (1) and (2) is a single-frequency solution of the form

$$Y=A\exp[i(\sigma-\omega)s] \tag{3}$$

and $Z=B$ where A, σ, and B are constants. It is called an ECM solution. Substituting Eq. (3) into Eqs. (1) and (2) leads to conditions for A, B, and σ. Specifically, the ECM frequency $\Delta\equiv\sigma\theta$ admits the implicit solution

$$\eta\theta=-\frac{\Delta-\omega\theta}{\alpha\cos(\Delta)+\sin(\Delta)} \tag{4}$$

and the intensity of each ECM is given by

$$A^2=\frac{P+\eta\cos(\Delta)}{1-2\eta\cos(\Delta)}\geqslant 0. \tag{5}$$

Using Eqs. (4) and (5), we may study how the ECM solutions appear as we progressively increase the feedback rate (see Fig. 1). Although Eq. (3) is an exact solution of Eqs. (1) and (2), a two-ECM solution of the form

$$Y=A_1\exp[i(\sigma_1-\omega)s]+A_2\exp[i(\sigma_2-\omega)s] \tag{6}$$

and $Z=B$ is not an exact solution of the LK equations. Nevertheless, it is the leading approximation of an asymptotic solution valid for large T [10]. This solution exists at and near critical points where two single ECMs admit the same intensity [10] (this point is indicated by an arrow in Fig. 1). This point is called a two-ECM point and is described analytically in the next section. Using Eq. (6), the intensity of the laser field is

$$|Y|^2=|A_1|^2+|A_2|^2+2|A_1||A_2|\cos[(\sigma_1-\sigma_2)s+\phi], \quad (7)$$

where ϕ is a phase. By contrast to the single-ECM solution (3), the intensity of the two-ECM solution (6) is oscillating with extrema $(|A_1|\pm|A_2|)^2$ and frequency $|\sigma_1-\sigma_2|$. In Refs. [10,12], we showed that this solution emerges from a first Hopf bifurcation located on a *stable ECM (mode)* and that it disappears at a second Hopf bifurcation located on an *unstable ECM (antimode)*. As a consequence, the two-ECM solution (6) is only stable near the first Hopf bifurcation. In this paper, however, we show that a branch of stable solutions connecting two *stable ECMs (modes)* is also possible.

As we shall demonstrate analytically in the following section, the stability of the two-ECM solutions depends on the location of the two-ECM point with respect to the saddle-node bifurcation point that creates the single-ECM solutions in pairs of mode and antimode. A direct investigation would be to determine analytically the stability of the two-ECM solutions. In order to investigate the stability of Eq. (6), we need to realize that in addition to the fast time of the ECMs (time s), the solution of the linearized equations depends on the slow time scales $T^{-1}s$ and $T^{-1/2}s$. The first slow time is obvious from Eqs. (1) and (2) since T appears in the left-hand side of Eq. (2) suggesting that Z is a function of $T^{-1}s$. The second slow time is motivated by the relaxation oscillation frequency of the solitary laser defined by $\omega_{RO}\equiv\sqrt{2P/T}$. It suggests introducing a slow time scaled by $T^{-1/2}$. The analysis is not a routine application of multiple scale methods [21,22] and will be described in detail elsewhere [23]. In the following section, we show that the location of the two-ECM point in parameter space is enough for anticipating two distinct bifurcation scenarios.

III. STABLE AND UNSTABLE BEATING BETWEEN TWO EXTERNAL-CAVITY MODES

Figure 1 illustrates a case where the two-ECM point is located on the low intensity part of the second ECM branch of solutions. It corresponds to an unstable ECM (antimode) [3]. A closed branch of two-ECM solutions connecting the first and second ECMs through Hopf bifurcation points is possible in the vicinity of this two-ECM point [10]. The first and second Hopf bifurcation points are then located on the stable and unstable ECMs, respectively. Consequently, the branch of two-ECM solutions connecting these points is stable only in the vicinity of the first Hopf bifurcation point.

We address now the following issue: Can the two-ECM point be located on the high intensity part of the second ECM branch of solutions, i.e., corresponding to a stable ECM (mode)? We shall examine this possibility in terms of the linewidth enhancement factor and show that this case is possible. A branch of stable two-ECM solutions connecting two stable bifurcation points is then possible.

The conditions for a two-ECM point is documented in Ref. [10]. The critical ECM frequencies Δ_1, Δ_2 satisfy the following conditions:

$$\Delta_1=\omega\theta-(\pi n-\Delta_1)[\alpha\cot(\Delta_1)+1], \quad (8)$$

$$\Delta_2=-\Delta_1+2\pi n, \quad (9)$$

where $n=\ldots-2,-1,1,2,\ldots$. The critical feedback rate is given by

$$\eta=\theta^{-1}\left(\frac{\pi n-\Delta_1}{\sin(\Delta_1)}\right)>0. \quad (10)$$

The case illustrated in Fig. 1 corresponds to $n=-1$. The intensity of the first ECM branch of solutions increases monotonically. But the intensity of the second ECM branch of solutions exhibits a limit or saddle-node bifurcation point. From this point emerges a stable and an unstable ECM solution. The lower part (the upper part) corresponds to the unstable (stable) solutions. The limit point satisfies the condition

$$d\eta/d\Delta=0 \quad (11)$$

and using Eq. (4), we obtain an equation for the ECM frequency at the limit point given by

$$\alpha\cos(\Delta)+\sin(\Delta)+(\omega\theta-\Delta)[\cos(\Delta)-\alpha\sin(\Delta)]=0. \quad (12)$$

A two-ECM point characterized by the two frequencies Δ_1 and Δ_2 may coalesce with a limit point of mode 2. To determine this point, we consider Eq. (8) with $\Delta_1=-\Delta_2+2\pi n$ and Eq. (12) with $\Delta=\Delta_2$. They represent two equations for Δ_2 and parameters α and $\omega\theta$. To determine the function $\alpha=\alpha(\omega\theta)$ for the two-ECM limit point, we proceed as follows. First we eliminate $\omega\theta$ from Eqs. (8) and (12):

$$\omega\theta=\Delta_2+(\pi n-\Delta_2)[\alpha\cot(\Delta_2)+1] \quad (13)$$

$$=\Delta_2-\frac{\alpha\cos(\Delta_2)+\sin(\Delta_2)}{\cos(\Delta_2)-\alpha\sin(\Delta_2)}. \quad (14)$$

After simplifying, we obtain a simple relation between α and Δ_2 given by

$$\alpha=\frac{1}{\sin(\Delta_2)}\left(\cos(\Delta_2)+\frac{\sin(\Delta_2)}{\pi n-\Delta_2}\right). \quad (15)$$

Using Eq. (13) for $\omega\theta=\omega\theta(\Delta_2)$ and Eq. (15) for $\alpha=\alpha(\Delta_2)$, we have the solution $\alpha=\alpha_c(\omega\theta)$ in parametric form $(-\pi<\Delta_2<\pi)$. The solution is displayed in Fig. 2.

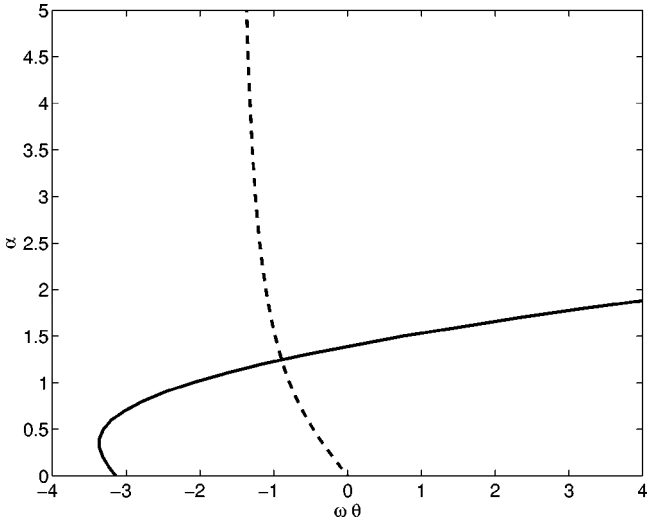

FIG. 2. Two-ECM limit point. The figure gives the critical value of α at which a two-ECM point coalesces with a limit point of single ECMs. $\alpha=\alpha(\omega\theta)$ is obtained using Eqs. (15) and (13) with $n=-1$. We use the same values of the laser parameters as in Fig. 1. The dotted line corresponds to the particular value $\omega\theta=-\arctan(\alpha)$ used for all our bifurcation diagrams. We note that α maximal value remains close to $\alpha=1$.

If we assume that $\omega\theta=-\arctan(\alpha)$ as in Refs. [7,10] (dotted line in Fig. 2), we find a specific value of α which is the root of

$$\frac{\alpha}{1-\alpha^2}=\pi n-\arctan(\alpha). \tag{16}$$

If $\alpha<\alpha_c$ ($\alpha>\alpha_c$), the two-ECM point is located on the stable part (unstable part) of the second ECM branch of solutions. Consequently, we may expect a stable bridge of solutions connecting the two single-ECM branches if α is sufficiently low. This hypothesis is investigated in the following section by determining the bifurcation diagrams of the stable steady and time-periodic intensity solutions for progressively smaller values of α.

IV. NUMERICAL BIFURCATION DIAGRAMS

In this section, we use a numerical continuation method specially developed for delay differential equations [11] and concentrate on the bifurcation diagram of the two first ECM solutions as η progressively increases. In addition to two single-ECM branches of solutions, we find a branch of two-ECM solutions that connects the two single-ECM branches. Because our numerical method allows the determination of stable and unstable solutions and marks all bifurcation points, we may observe how the closed branch of two-ECM solutions gradually stabilizes as we decrease α and as it passes α_c.

We first consider the case $\alpha>\alpha_c$; see Figs. 3(a–c). The first mode exhibits a Hopf bifurcation (indicated by a diamond in Fig. 3) that gives rise to a time-periodic solution. This time-periodic solution corresponds to a two-ECM solution, with a frequency given by $|\sigma_1-\sigma_2|/2\pi$, in first approximation. σ_1 and σ_2 are the frequencies of the two ECMs whose intensities are equal at the two-ECM point. The two-ECM solution then changes stability through a torus bifurcation point (indicated by a square in Fig. 3). At the torus bifurcation point a new frequency appears that is proportional to the laser relaxation oscillation frequency, i.e., is an $O(T^{-1/2})$ small quantity. Our continuation method allows to follow the two-ECM solution when it becomes unstable (shown in dashed line). We find that the branch of two-ECM time-periodic dynamics ends at a Hopf bifurcation point on an antimode. Modes and antimodes are therefore connected through a Hopf bifurcation bridge and the dynamics observed along the bridge corresponds to a mixed ECM solution [10,12].

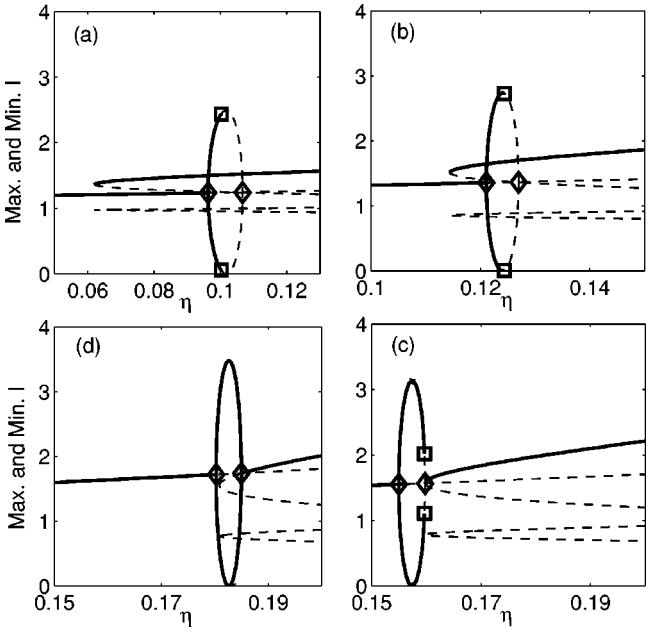

FIG. 3. Numerical bifurcation diagram of the single and two-ECM solutions. Each figure represents the extrema of the intensity $I\equiv|Y|^2$ as a function of η. Full and broken lines correspond to stable and unstable solutions, respectively. The stable and unstable solutions of Eqs. (1) and (2) have been obtained by using a continuation method. The value of α is given by (a) $\alpha=4$, (b) $\alpha=2$, (c) $\alpha=1.25$, and (d) $\alpha=1$. The values of the fixed parameters P, θ, $\omega\theta$ are the same as in Fig. 1 and $T=1710$. All figures show a closed branch of two-ECM solutions connecting two Hopf bifurcation points (diamonds). This branch changes stability at a torus bifurcation point (square). The torus bifurcation point progressively moves to the right Hopf bifurcation point as α progressively decreases. In Fig. 3(d) the closed branch of two-ECM solutions is stable.

Figure 4 shows a typical quasiperiodic output for the laser intensity $I\equiv|Y|^2$ and the field phase difference $\phi(s)-\phi(s-\tau)+\omega\theta$. A slow modulation of the intensity oscillations appears at the relaxation oscillation frequency given by $f_{RO}\equiv\sqrt{2P/T}/2\pi$. For the parameters considered in Fig. 3, it corresponds to $f_{RO}\sim 5.85$ GHz if $\tau_p=1$ ps.

Figure 5 shows the optical spectra for the dynamical behaviors that characterize the Hopf bifurcation bridge between a mode and an antimode. As we gradually increase the feedback rate, the first ECM (a) destabilizes to a two-ECM dynamics (b) and then quasiperiodic oscillations occur (c). We

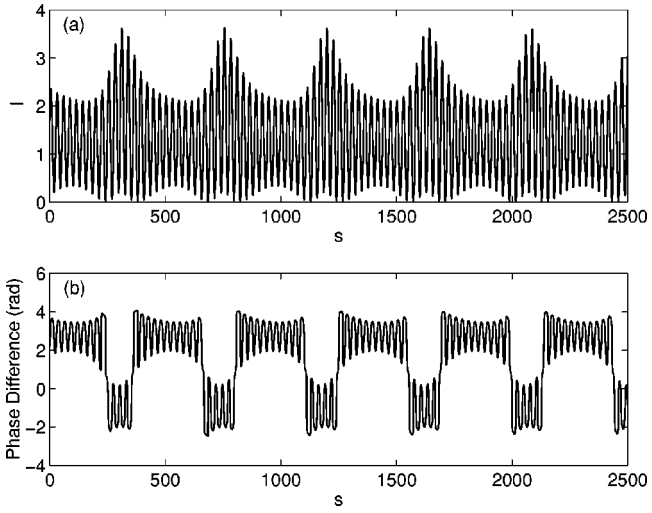

FIG. 4. Quasiperiodic dynamics after a torus bifurcation point of the two-ECM solution. The parameters are the same as in Fig. 3(b) and the feedback rate is $\eta=0.125$. Figure 4(a) shows the laser intensity $I=|Y|^2$ as a function of time s while Fig. 4(b) shows the evolution of the field phase difference variable $\phi(s)-\phi(s-\tau)+\omega\theta$. Note that it periodically switches between rapid oscillations located near one of the two single-ECM frequencies.

see clearly that the microwave oscillations involve two-ECMs, but only the highest frequency peak which corresponds to a mode can be isolated in Fig. 5(a). The lowest frequency peak corresponds to an antimode, which is unstable and therefore not available to experiment and/or direct numerical integration of the rate equations. As the two-ECM solution changes stability to a quasiperiodic output, side peaks appear around the main beating ECMs, with a frequency separation between the side and the main peaks approximately corresponding to f_{RO}. The recent experiments on double cavity feedback [15] are relative to bifurcation bridges between a mode and an antimode, similar to what is shown in Fig. 3(a–c), and the transition between the two-ECM dynamics and the quasiperiodic behavior as presented in the optical spectra of Fig. 5(a–c) has been confirmed experimentally in Ref. [15].

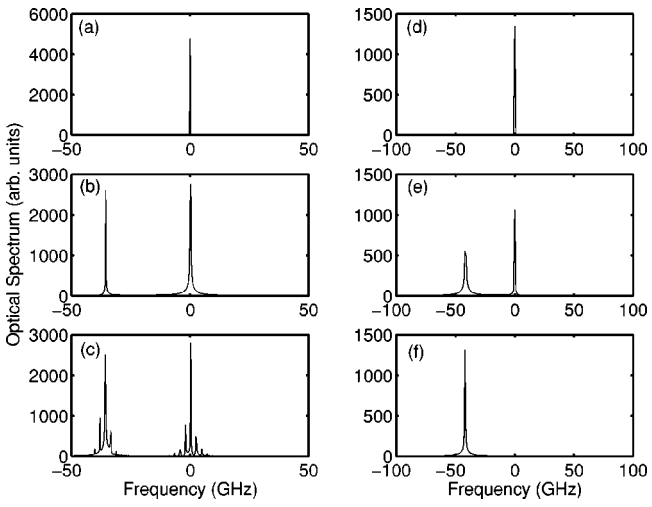

FIG. 5. Optical spectra. In the left column, the spectra correspond to a mode-antimode bridge. The values of the parameters are the same as in Fig. 3(b), with $\tau_p=1$ ps, and (a) $\eta=0.12$, (b) $\eta=0.123$, (c) $\eta=0.125$. Figures 5(a)–5(c) illustrate the typical spectrum of a single ECM, a two-ECM, and a torus regime, respectively. In the right column, the spectra correspond to a stable mode-mode bridge. The values of the parameters are the same as in Fig. 3(d), with $\tau_p=1$ ps, and (d) $\eta=0.18$, (e) $\eta=0.182$, (f) $\eta=0.185$. Figures 5(d)–5(f) illustrate the spectrum of the first single ECM, the two-ECM solution, and the second single ECM.

When α decreases, the two-ECM point becomes closer to the saddle-node bifurcation point that creates the pair of mode and antimode until it merges with this limit point for $\alpha=\alpha_c$. As α passes through α_c, the two-ECM point is now located on a mode branch; see Fig. 3(d). The torus bifurcation point disappears giving rise to a stable branch of solutions connecting two stable ECM solutions. Figure 5(e) shows the optical spectrum for the two-ECM solution. When we decrease the feedback, we isolate the highest frequency peak, which corresponds to the first mode [see Fig. 5(d)]. On the other hand, increasing the feedback rate isolates the lowest frequency peak, which corresponds to the second beating mode [see Fig. 5(f)]. By contrast to the situation depicted in Fig. 5(a–c), both beating ECMs can be isolated in the optical spectra and quasiperiodic oscillations do not occur.

V. DISCUSSION

To summarize, we have performed a bifurcation analysis of the LK equations and shown that stable microwave oscillations can be generated in a semiconductor laser subject to optical feedback. These high-frequency time-periodic intensities correspond to a two-ECM solution of the LK equations and result from a beating between two stable ECMs (or modes). The stability of the microwave oscillations has been analyzed in an asymptotic expansion of the LK equations valid for large ratio between carrier and photon lifetime, and the validity of our theoretical assumptions has been checked through numerical computations of stable and unstable time-periodic solutions. The main conclusion is that stable two-ECM solutions (and therefore stable microwave oscillations) are possible for a sufficiently low α factor ($\alpha\leqslant\alpha_c\simeq 1$).

Low α factors are desirable since they improve the intensity modulation characteristics and reduce the chirp. The α factor depends on the detuning between the emission wavelength and the material gain peak. In Fabry-Perot type lasers the emission wavelength is given by the gain peak and the control of α to a large extent is difficult. But distributed-feedback-type lasers or VCSELs for example emit at a wavelength that is determined by the grating period and the laser design, and can strongly be detuned from the gain peak. The α factor can be further reduced using multiple quantum wells in the active region [24] or strain effects in the energy bands [25]. It is worth noting that the influence of the α factor on the dynamics of semiconductor lasers subject to optical feedback has been recently examined experimentally for long

cavities [26,27], i.e., for external cavity round-trip time much larger than the relaxation oscillation period. We show here that the reduction of the α factor can transform the short cavity induced instabilities into efficient sources of microwave oscillations.

Our results motivate further investigations in other external-cavity configurations that might simplify the generation of these microwave oscillations. Indeed, more complicated feedback systems such as double external cavities [13-15] or two-polarization laser systems [16–18] will increase the number of two-ECM points around which two-ECM solutions appear.

ACKNOWLEDGMENTS

This research was supported by the Fonds National de la Recherche Scientifique (FNRS, Belgium), the InterUniversity Attraction Pole (IAP V/18) program of the Belgian government, the US Air Force Office of Scientific Research Grant No. AFOSR F496, 20-98-1-0400, and the National Science Foundation Grant NO. DMS-9973203.

[1] D. Lenstra, B.H. Verbeek, and J. den Boef, IEEE J. Quantum Electron. **QE-21**, 674 (1985).
[2] J. Mork, J. Mark, and B. Tromborg, Phys. Rev. Lett. **65**, 1999 (1990).
[3] J. Mork, B. Tromborg, and J. Mark, IEEE J. Quantum Electron. **QE-28**, 93 (1992).
[4] Y. Cho and T. Umeda, Opt. Commun. **59**, 131 (1986).
[5] H. Li, J. Ye, and J.G. McInerney, IEEE J. Quantum Electron. **29**, 2421 (1993).
[6] A.A. Tager and B.B. Elenkrig, IEEE J. Quantum Electron. **QE-29**, 2886 (1993).
[7] A.A. Tager and K. Petermann, IEEE J. Quantum Electron. **QE-30**, 1553 (1994).
[8] R. Lang and K. Kobayashi, IEEE J. Quantum Electron. **QE-16**, 347 (1980).
[9] K. Petermann, IEEE J. Sel. Top. Quantum Electron. **1**, 480 (1995).
[10] T. Erneux, F. Rogister, A. Gavrielides, and V. Kovanis, Opt. Commun. **183**, 467 (2000).
[11] K. Engelborghs, DDE-BIFTOOL: a MATLAB package for bifurcation analysis of delay differential equations, http://www.cs.kuleuven.ac.be/~koen/delay/ddebiftool.shtml
[12] D. Pieroux, T. Erneux, B. Haegeman, K. Engelborghs, and D. Roose, Phys. Rev. Lett. **87**, 193901 (2001).
[13] F. Rogister, P. Mégret, O. Deparis, M. Blondel and T. Erneux, Opt. Lett. **24**, 1218 (1999).
[14] F. Rogister, D.W. Sukow, A. Gavrielides, P. Mégret, O. Deparis, and M. Blondel, Opt. Lett. **25**, 808 (2000).
[15] D.W. Sukow, M.C. Hegg, J.L. Wright, and A. Gavrielides, Opt. Lett. **27**, 827 (2002).
[16] H. Li, A. Hohl, A. Gavrielides, H. Huo, and K.D. Choquette, Appl. Phys. Lett. **72**, 2355 (1998).
[17] M. Sciamanna, T. Erneux, F. Rogister, O. Deparis, P. Mégret, and M. Blondel, Phys. Rev. A **65**, 041801(R) (2002).
[18] M. Sciamanna, F. Rogister, O. Deparis, P. Mégret, M. Blondel, and T. Erneux, Opt. Lett. **27**, 261 (2002); **27**, 875(E) (2002).
[19] T. Erneux, Proc. SPIE **3944**, 588 (2000).
[20] P.M. Alsing, V. Kovanis, A. Gavrielides and T. Erneux, Phys. Rev. A **53**, 4429 (1996).
[21] C.M. Bender and S.A. Orszag, *Advanced Mathematical Methods for Scientists and Engineers* (McGraw-Hill, New York, 1978).
[22] J. Kevorkian and J.D. Cole, *Perturbation Methods in Applied Mathematics*, Applied Mathematical Sciences Vol. 34 (Springer, New York, 1981); *Multiple Scale and Singular Perturbation Methods*, Applied Mathematical Sciences Vol. 114 (Springer, New York, 1996).
[23] T. Erneux, A. Gavrielides, and M. Sciamanna (in preparation).
[24] C.A. Green, N.K. Dutta, and W. Watson, Appl. Phys. Lett. **50**, 1409 (1987).
[25] Y. Hirayama, M. Morinaga, M. Tanimura, M. Onomura, M. Funemizu, M. Kushibe, N. Suzuki, and M. Nakamura, Electron. Lett. **27**, 241 (1991).
[26] T. Heil, I. Fischer, and W. Elsässer, Phys. Rev. A **60**, 634 (1999).
[27] T. Heil, I. Fischer, and W. Elsässer, J. Opt. B: Quantum Semiclassical Opt. **2**, 413 (2000).